MMAN4410 T3 - Finite Element Methods

Final Report

'Modelling of a carbon fibre composite off-the-shelf prosthetic sprinting foot.'

Name: Maximilian Keller
zID: z5265207
Date of Submission: 21/11/2021

Executive Summary

This report employs the Finite Element Analysis (FEA) software package ANSYS to investigate the stresses experienced by a performance prosthetic sprinting foot under extreme loading conditions and optimise its construction with carbon-fibre composite material. Preliminary research was conducted into the various categories of prosthetic lower limbs, with the Energy Storing and Return (ESR) category considered in this investigation. An off the shelf "J-blade" type carbon-fibre running prosthetic was chosen made by the Icelandic company *Össur*, as this was found to be one of the most popular performance running prosthesis on the market. A replica Computer Aided Design (CAD) model of the *Össur Cheetah® Xcel* foot was constructed using the dimensions and geometry given in the technical manual for the device.

Various meshing strategies were tested to convert the CAD geometry into a discretised representation of the prosthesis. Shell-type elements were found to converge to a constant solution with the smallest number of mesh elements and could represent the stresses in the geometry most accurately given the limitations of the ANSYS student licence. Furthermore, various boundary conditions were tested. The final boundary and loading conditions were successfully validated with high accuracy through hand calculations, showing only small discrepancies to the expected theoretical result. The FEA model was validated in a static structural analysis using an isotropic aluminium alloy. The loading case was justified through existing research on the forces subjected to performance prosthetics, and the maximum normal loading scenario was investigated thoroughly.

Given the successful preliminary studies to verify and validate the finite element model of the prosthetic foot, the analysis was extended to ANSYS Composite PrepPost (ACP) to analyse the construction of the foot with carbon fibre composite material. The original Össur Cheetah® Xcel foot is constructed using pre-impregnated (pre-preg) carbon fibre fabric, which is then baked in an autoclave oven. Hence, this investigation also considered pre-preg material to simulate the construction of the Össur foot.

Two different fabric types were considered in this investigation including *Epoxy Carbon Woven (230GPa) Prepreg (0.2mm)* and *Epoxy Carbon Unidirectional Prepreg (0.2mm)*. Many different layup arrangements and combinations were trialled and analysed by paramterising the number of carbon plys in various locations. Parametrisation of the inputs and stress response of the model made it possible to test many design iterations and arrive at an optimum design.

The results showed that quasi-isotropic twill plys could uniformly distribute the bending stresses across the width of the carbon blade, whereas the unidirectional fibre performed better at carrying the bulk of the axial loads along the outer edges of the carbon blade. However, the unidirectional fibre showed premature failure along the edges of the part. The best overall strength to weight ratio could be seen by staggering fabric inside the curvature of the blade where the most stress is experienced in order to reinforce the blade in its failure zone.

Table of Contents

Table of Figures

1. Introduction

During the 2016 Rio de Janeiro Olympics, long jump runner Markus Rehm was denied being able to compete as he was not able to prove to the committee that his carbon-fibre running prosthetics did not give him an unfair advantage against able-bodied athletes. This situation is fascinating, considering that one would assume an amputee is inherently disadvantaged to regular athletes. Continuous research is being done on this category of prosthetic running foot known as Energy Storing and Return (ESR) prosthetics which are aimed at storing energy during mid-stance motion and maximising the energy recovery during late-stance motion. However, the exact impact on performance is still being disputed [1]. Hence, the focus of this investigation is to model and analyse ESR prosthetic running blade and potentially gain some insight into how these prosthetics function.

Figure 1 Amputee Oscar Pistorius in his ESR prosthetic running blades.

The use of carbon Fibre Reinforced Polymers (CFRPs), or simply *carbon fibre* is widespread amongst the market for high-performance engineering structures due to several inherent advantages over traditional monolithic materials. Such advantageous include high tensile strength, high stiffness, light weight, high temperature tolerance, high chemical resistance and low thermal expansion. However, unlike common building materials such as metals or plastic which are classified as isotropic materials, meaning their mechanical properties are the same in all directions, CFRP is an anisotropic material. CFRP are a combination of two different materials, the first being the carbon reinforcement. It consists of long, thin fibres (even smaller than the thickness of human hair) of carbon which are bundled together in thousands into what is known as a tow. Tows are woven together into fabrics which form the distinguishing tessellating checkered pattern. The second part of CFRP is the polymer matrix which provides shape and holds the carbon fibres in place by transferring loads short distances between adjacent fibres [2]. Thermoset plastics such as two-part epoxy resins or polyester are commonly used as matrix components. The composite nature of CFRP leaves

the cured material strongest in the direction of the carbon fibres but weakest between adjacent fibres held together by the matrix agent. This anisotropy provides added freedom to the engineer as the carbon fibre reinforcement can be arranged according to the loading directions in the desired structure [3]. However, the selective orientation of fibres in designs requires a more thorough understanding of the loading scenario and becomes very complex when many different fabric types are incorporated. Finite Element Modelling (FEM) can be used to effectively simulate the stresses and strain energy developed in such prosthetic devices.

2. Aim

The aim of this investigation is to accurately model and simulate the stresses in a composite ESR carbon fibre running blade prosthesis using the ANSYS Composite PrepPost (ACP) and optimise the construction and weight of such a prosthesis. A simplified model of a popular off-the-shelf running prosthesis will be considered in keeping to the scope of this investigation.

3. Model Definition

Translating the real-world problem into a CAD geometry started by researching existing off-the-shelf prosthetic running blade. The brand Össur™ offers a range of prosthetic devices and feet, with part of their range being performance blades such as the ones shown in figure 2.

Figure 2 Various models of Össur™ prosthetic performance blades - Cheetah® Xpanse (left), Cheetah® Xcel (middle), Cheetah® Xceed (right).

These blades were chosen for their mechanical simplicity yet interesting geometry. The left model is considered a long jumping blade, the middle a high performance short-distance sprinting blade, and the right being an everyday sport enthusiast blade. I chose the middle as this is the style of blade which allows athletes to match able-bodied person's records and it also holds the most interesting curvature.

The side profile of the Xcel blade from the manufacturer website was imported into fusion 360 as a canvas such that it could be traced onto a sketch. Originally this was done using a single spline curve for each edge, however this left undesirable geometry. Hence, the sketch was modelled as a series of circular arcs, line section and splines joining these features.

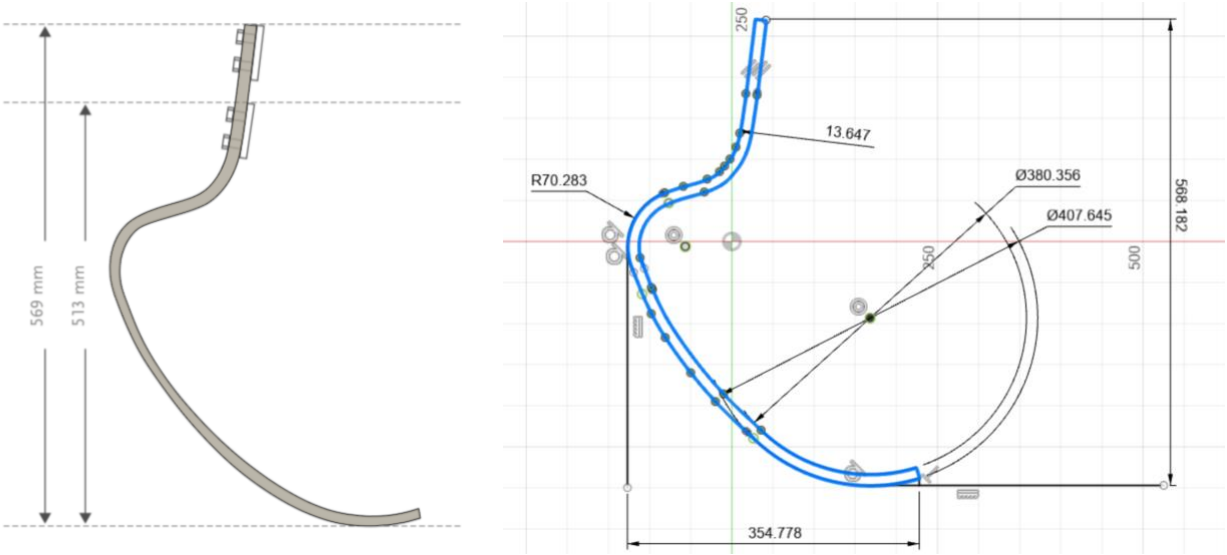

Figure 3 Fusion 360 sketch of blade profile based off proportions given by manufacturer

As shown in the left of figure 3, the original design uses variable thickness to achieve the desired mechanical characteristics, however the final sketch was approximated and extruded as a uniform thickness as shown in figure 4. An L-shaped bolt-on adapter was also modelled as a separate component using the proportions given in the OSSUR technical manual which makes a 13˚ angle to the vertical such that the foot propels the user slightly forward when running [4]. The L – bracket attaches to a standard 4-hole titanium 'pyramid style' connector which connects to the prosthetic limb (shown in figure 4). The CAD model was then simplified into a surface body (along with the ground plane) and the face was cleaned up in Design Modeller.

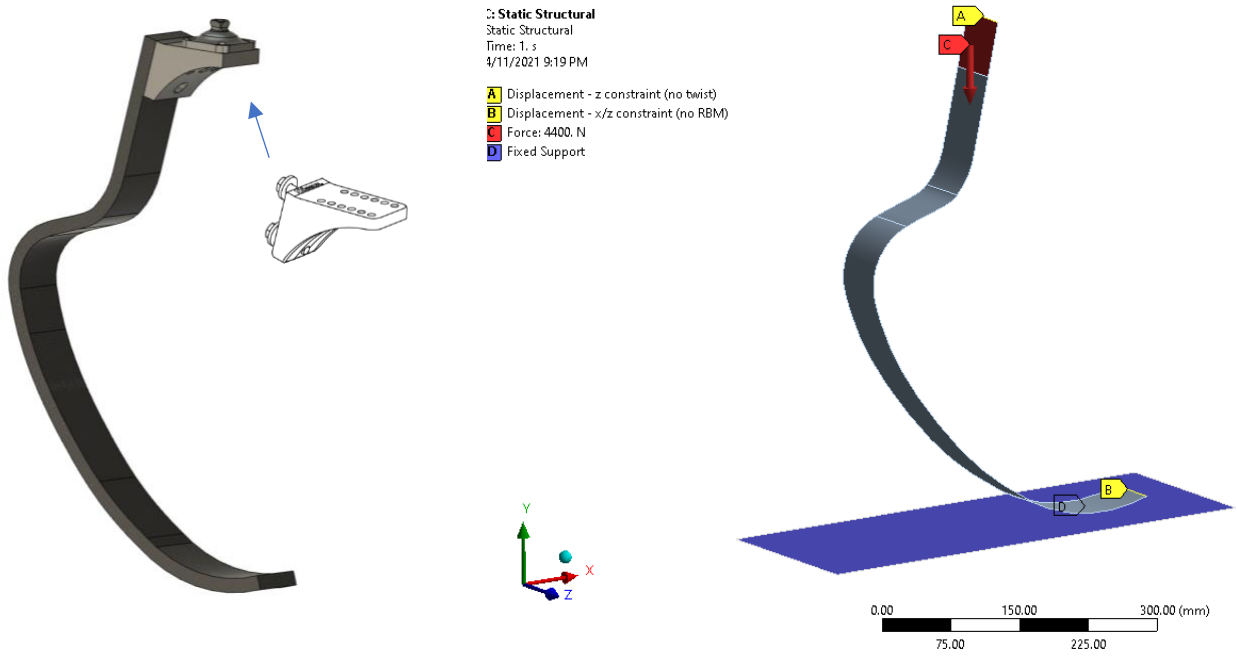

Figure 4 The final CAD geometry (left) and simplification to surface body in ANSYS (right)

Boundary Conditions:

The contact region of the L-bracket on the blade was split into a separate face to which the force exerted by the runner could be applied. Although this is a simplification, the manufacturer recommends a tight torque and adhesive to bold the adapter to the blade, which can justify applying the load to the entire face of contact. Furthermore, the ground was modelled as a fixed support surface with a frictionless contact, allowing the blade to slide along the ground plane as it deforms. A preliminary study was done where a few elements on the blade adjacent to the ground where fixed in space without modelling the ground plane, however this resulted in stress concentrations at the support and results which did not agree with general existing research [5]. Additionally, free movement in the x-direction (figure 4) between the bottom and top of the blade is a justifiable assumption as the runner is not rigidly attached to the ground in any way. Lastly, the top edge of the blade was constrained from moving in the z direction (to prevent twisting), whilst the bottom edge was constrained in x and z to prevent Rigid Body Motion.

4. Numerical Approach and Verification

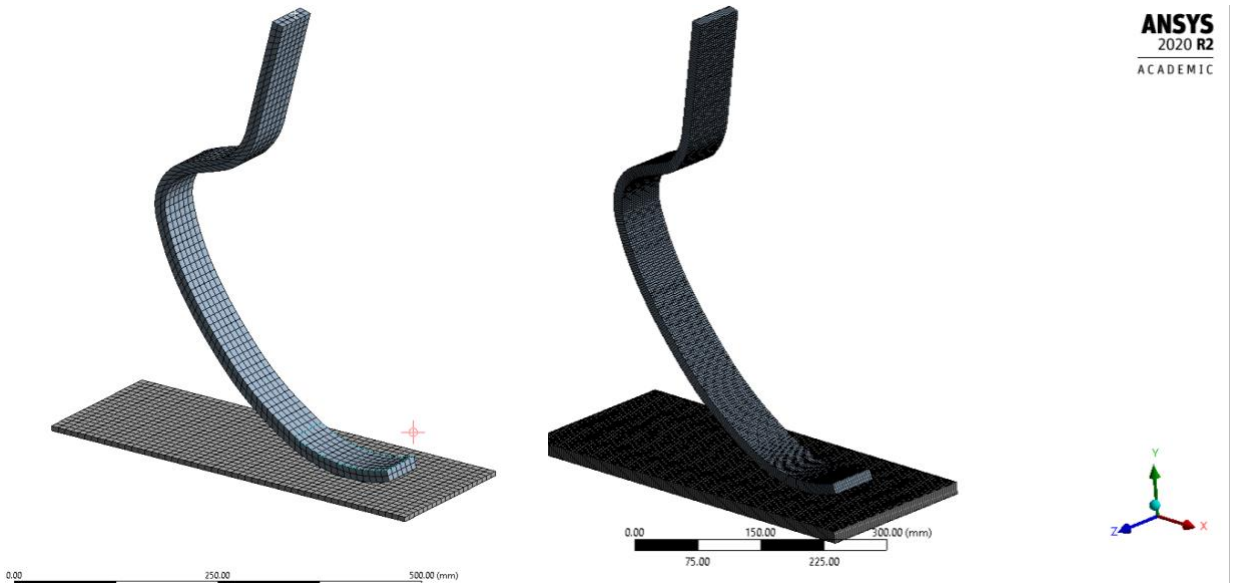

Figure 5 Meshing of CAD model using solid hexahedral elements (left) and shell elements (right)

A preliminary test was conducted using the 3D CAD model with solid hexahedral (hex) mesh elements (left of figure 5). This was done as an alternative option to the shell elements using the surface body, as shown in the right of figure 5. The ANSYS student licence would not allow a smaller mesh for the hex elements (smaller than two elements in thickness). However, it is generally recommended to use a minimum of four elements through the thickness of a structure to model bending with solid elements [6]. On the contrary, shell elements can much more efficiently model the bending of the blade, with the ANSYS licence allowing a mesh size of less than 3mm. This made shell elements the obvious choice for this study.

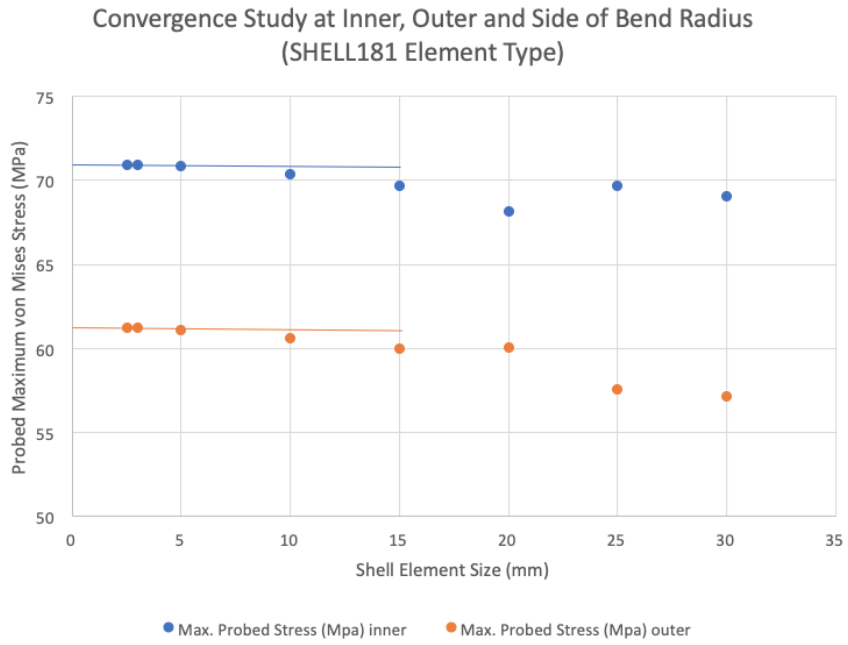

Figure 6 Mesh convergence study.

Using the shell element mesh, a mesh convergence study was carried out with a sample load of 1000N to ensure that the stress at one point on the inside and outside of the main curvature of the blade does converge using the shell mesh elements. As illustrated in figure 6, the mesh size was decreased from 30mm to 2.5mm, showing convergence from approximately 5mm mesh sizing. A 3mm mesh size was selected as appropriate as this was closest to the converged value without taking excess computational time. The 3mm mesh will be used for the remainder of this report.

5. Preliminary Validation

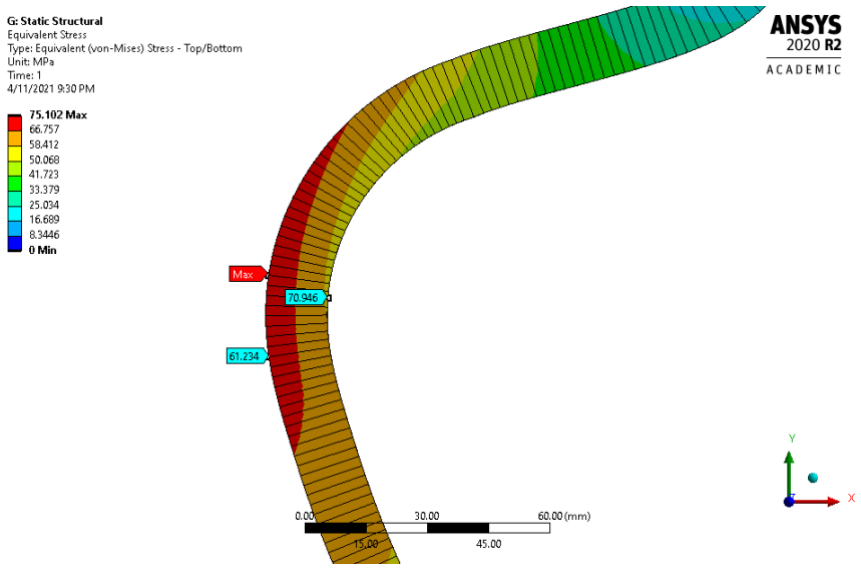

Figure 7 Preliminary stress analysis using isotropic aluminium for validation purposes

A preliminary stress analysis was done using the 3mm shell element mesh and using isotropic aluminium as a material to validate the model set up and boundary conditions. A force of 1000N was applied and the von Mises stress was probed in the inside (σ_i) and outside (σ_o) face of the circular bend section of the blade as illustrated in figure 7. The loading is approximately equivalent to a 100kg person standing on one foot and is chosen as a benchmark to verify the mesh. Although the loading force will be altered slightly in the latter sections of this report, the mesh and boundary conditions will remain the same and hence, this study serves as preliminary validation of the boundary conditions and discretisation applied to the model. The theoretical stress in this section of the blade could be calculated by considering the bending stress for a beam with uniform circular radius and cross section and adding the contribution of axial stress throughout the member. This technique is a justified approach at calculating the stress in the circular section of the blade because the CAD geometry is modelled using perfectly circular arcs to approximate the shape of the Össur foot. Detailed calculations can be found in Appendix A.

Total Theoretical	σ_i (MPa)	75.3
	σ_o (MPa)	67.3
Total Simulated	σ_i (MPa)	70.9
	σ_o (MPa)	61.2
Error (%)	σ_i	5.80%
	σ_o	8.99%

Table 1 Comparison of Stress values at the middle of the curved blade section.

The theoretical results were very close to the probed stress values, with a deviation of only 5.80% and 8.99%. These results are very similar considering that the theoretical bending stress is an approximation for a single beam with perfect circular curvature. Furthermore,

the stress was probed as the maximum stress at the centre of the beam curvature, however there are noticeable fringe effects on the sides of the blade, which is where the maximum stress concentration occurs (as shown in figure 8). These fringe effects can be expected as stress concentrations arise along the sharp edges without adjacent elements to distribute stress. However, this makes it more difficult to compare theoretical values. The middle was chosen as a probe point to stay away from these 'fringe' effects.

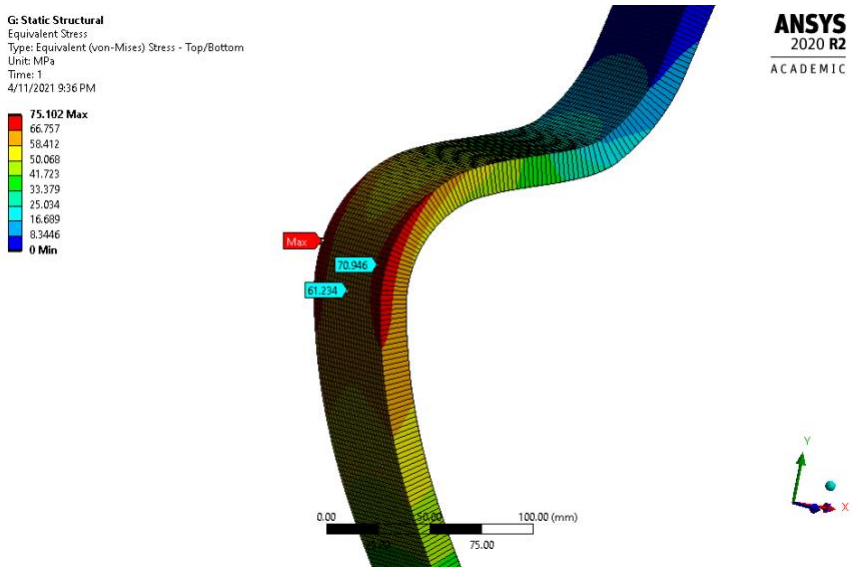

Figure 8 Preliminary Stress Analysis showing Fringe Benefits

6. Results

Knowing that the applied mesh accurately discretised the 3D model using the convergence study and the applied boundary conditions are valid, the model was transferred to ACP. The two fabric types used in the study included *Epoxy Carbon Woven (230GPa) Prepreg (0.2mm)* and *Epoxy Carbon Unidirectional Prepreg (0.2mm)*. As this study is primarily focussed on the process of optimising the composite laminate model, additional fabrics were not considered. The pre-preg consists of a reinforcement material which is pre-impregnated with an epoxy resin matrix. Pre-preg fibre parts are placed in an autoclave to cure at high pressure and heat, which is the method used in the manufacturing of the Ossur foot which the CAD model is based on. Hence, pre-preg was also chosen for this study. The first stackup considered was a $[0/45]_n$, where the number of times the pattern repeats itself, n, was parameterised. This is a common pattern used with regular twill to form quasi-isotropic parts [7]. A parametric study was used to compare the number of layers to the max stress and factor of safety using the max-stress failure criteria.

Design Number	Number of [0/45] laminae	Max Stress (Pa)	Safety factor	Total Thickness (mm)
DP 0	8	8727.5	-0.942	3.2
DP 1	30	678.3	-0.249	12
DP 2	40	373.5	0.346	16
DP 3	50	233.5	1.124	20
DP 4	55	190.8	1.583	22
DP 5	60	158.5	2.089	24

Table 2 Parametric study 1 - 0/45 layup

For most high performance prosthetic limbs, a safety factor (SF) between 1 and 2 is generally regarded as acceptable, with papers often adopting a SF between 1 and 1.5 [8], [9]. The study showed that about 50-55 laminae are required to achieve a safety factor of about 1.1-1.6, giving a total thickness of about 20-22mm. All tests were carried out using a 4400N load applied directly to the top face of the blade which is to be bonded to the L-bracket adapter (as depicted in figure 5). A 4400N load was chosen as this is approximately 3 times the weight force of a 147kg runner, which is the maximum design capacity of the Ossur Cheetah Xcel model [10]. Three times this force was used because this is the maximum normal force a sprint runner will experience [11]. As such, this should serve as the maximum loading case that the foot may experience. It was assumed that no external moments are applied to the blade by the runner, as there is no rigid attachment to the ground, and based on existing research on similar prosthetic blades, this assumption is justifiable.

As expected, the maximum tensile and compressive stresses were exhibited in the outermost 0-degree and innermost 0-degree plies, with a similar stress concentration to that seen in the preliminary isotropic study (as illustrated in figure 9 on the following page). Due to the outer and innermost fibres being under the most amount of stress, this is also the region were failure is most likely to occur. This particular stress distribution was also expected based on the theoretical calculations and analysis (Appendix A).

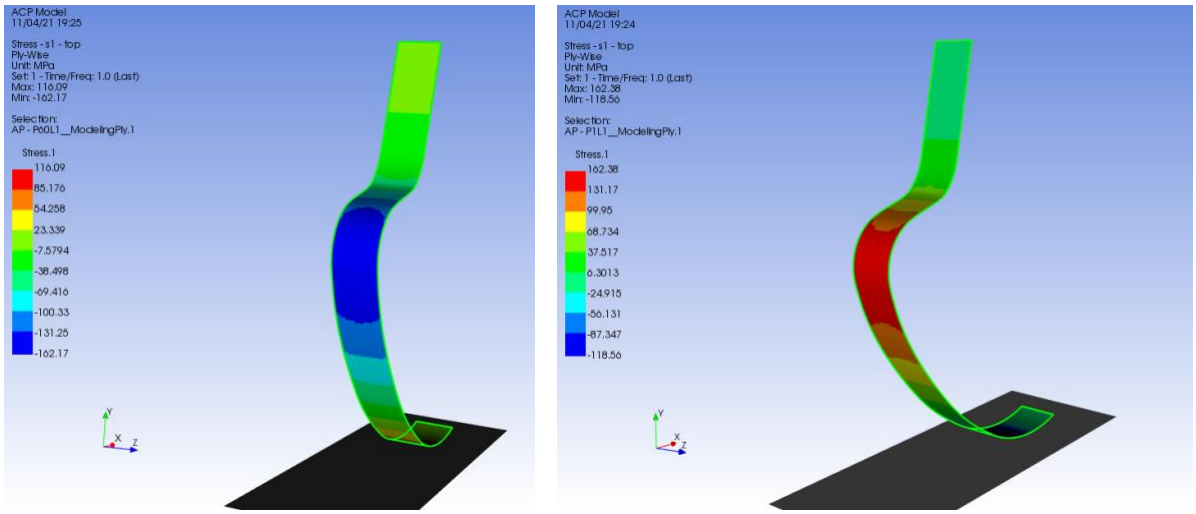

Figure 9 ACP results for 0/45 ply with 60 repetitions at outer (left) and inner (right) edges

Following this study, a second layup pattern was introduced using the uni-directional fibre in a $[-30/0/30]_n$ pattern. The number of repetitions was again parametrised as an input. The width of the blade was also initially parametrised as an input in ANSYS Design Modeller, to find the best balance between width and layup number. However, the width of the blade was later decided to be constant and equal to the width of the original blade.

Design Number	Number of [-30/0/30] laminae	Max Stress (MPa)	Safety factor	Total Thickness (mm)
DP 0	50	125.9	3.32	30.0
DP 1	45	158.5	2.52	27.0
DP 2	42	184.1	2.08	25.2
DP 3	40	204.5	1.81	24.0
DP 4	38	228.3	1.55	22.8
DP 5	37	241.6	1.42	22.2
DP 6	35	271.9	1.18	21.0
DP 7	33	307.8	0.95	19.8
DP 8	32	328.2	0.84	19.2
DP 9	30	375.4	0.63	18.0

Table 3 Parametric study 2 - -30/0/30 layup

Surprisingly, the unidirectional performed slightly worse than the [0/45] ply, given total thickness. It was expected that with more fibres running in the direction of the bending stress vector, that more bending stress can be supported. Figure 10 shows the stress distribution a -30 degree and 0-degree inner fibre. The 0-degree fibre shows similar fringe effects to the isotropic study, whereas the 30-degree fibre shows an uneven stress distribution along the direction of its fibres.

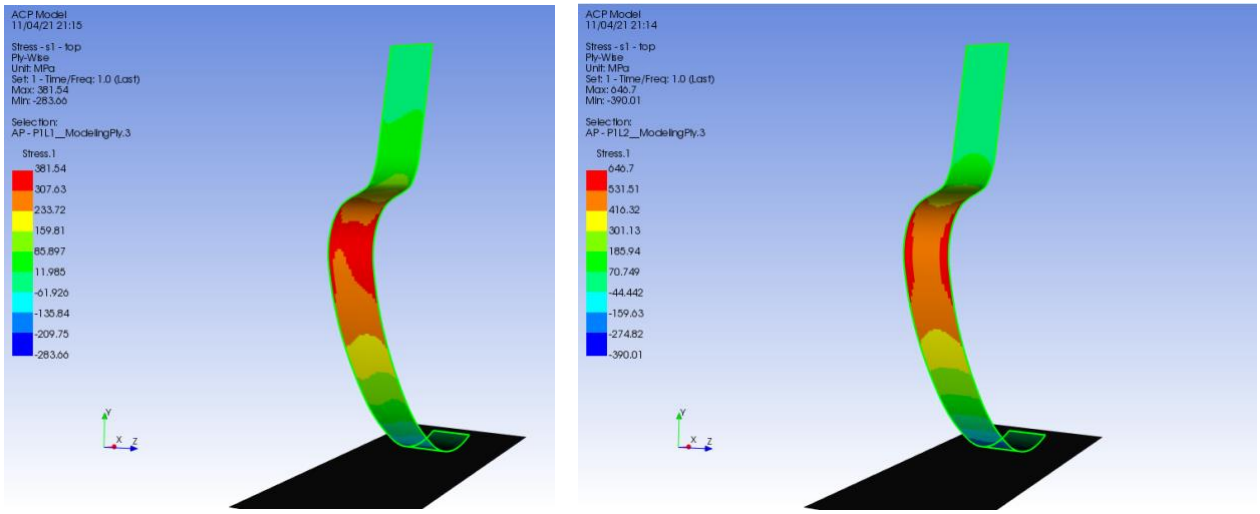

Figure 10 ACP results for -30/0/30 ply with 30 repetitions at inner -30 degree fibre (left) and 0 degree fibre (right).

The reason as to why the unidirectional fibre seems to underperform when compared to the first study involving the [0/45] twill is related to the fringe effect stresses seen on the edge of the blade. Figure 12 shows a comparison of the outermost layer of 0-degree oriented fabric from the [0/45] ply (left) and the [-30/0/30] ply right.

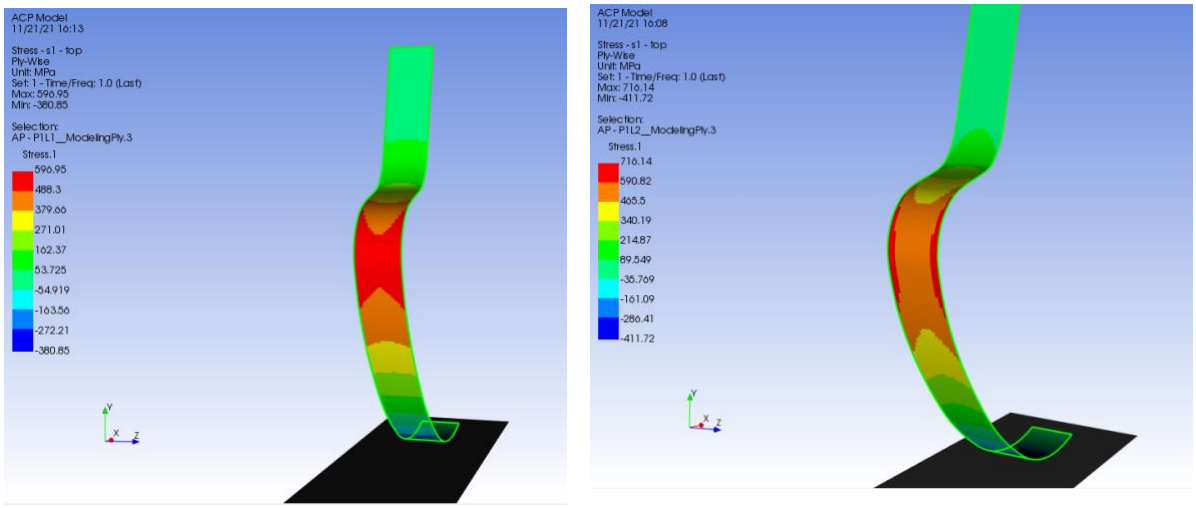

Figure 11 Comparison of stress distribution in unidirectional fabric (right) and twill fabric (left)

In the twill fabric, the highest stress area has a more uniform stress distribution along the width of the blade in red (with the maximum stress being lower than the UD fabric at 597 MPa) whereas the unidirectional fibre has higher stress on the edges of the blade (716MPa), albeit a lower average maximum stress along the inside of the blade (500MPa). This is an interesting result, and likely due to the orthogonal pulls of carbon fibre in the twill fabric allowing the load to be evenly spread along the width of the blade.

The next study combines the results seen in the previous two, by sandwiching a 12 layers of the quasi-isotropic twill [0/45] ply between two evenly split sections of unidirectional [-30/0/30] ply. The total number of unidirectional triplets (n) were parameterised again such

that the entire model followed the pattern: $[-30/0/30]_{n/2}$, [0/45], $[-30/0/30]_{n/2}$. The following results were obtained from this parametric study.

Design Number	Blade Width (mm)	Total Number of [-30/0/30] laminae	Max Stress (MPa)	Safety factor	Total Thickness (mm)
DP 0	60	20	646.7	0.496	16.8
DP 1	60	30	393.1	1.650	22.8
DP 2	60	40	263.7	3.069	28.8
DP 3	60	50	189.0	4.547	34.8
DP 4	60	60	141.9	6.243	40.8

Table 4 Parametric Study 3 - $[-30/0/30]_{n/2}$, [0/45], $[-30/0/30]_{n/2}$

When considering the Total thickness of the blade in comparison to the maximum stress or safety factor, this study showed no considerable increase in performance compared to the previous two studies. At this point, it became clear that a staggered layup is required to give the blade more support in the sections were failure is likely to occur, without increasing the global thickness and weight of the blade. The original Ossur blade is also noticeably uneven in thickness along its length, and hence a similar staggering technique is likely to be used for its manufacture.

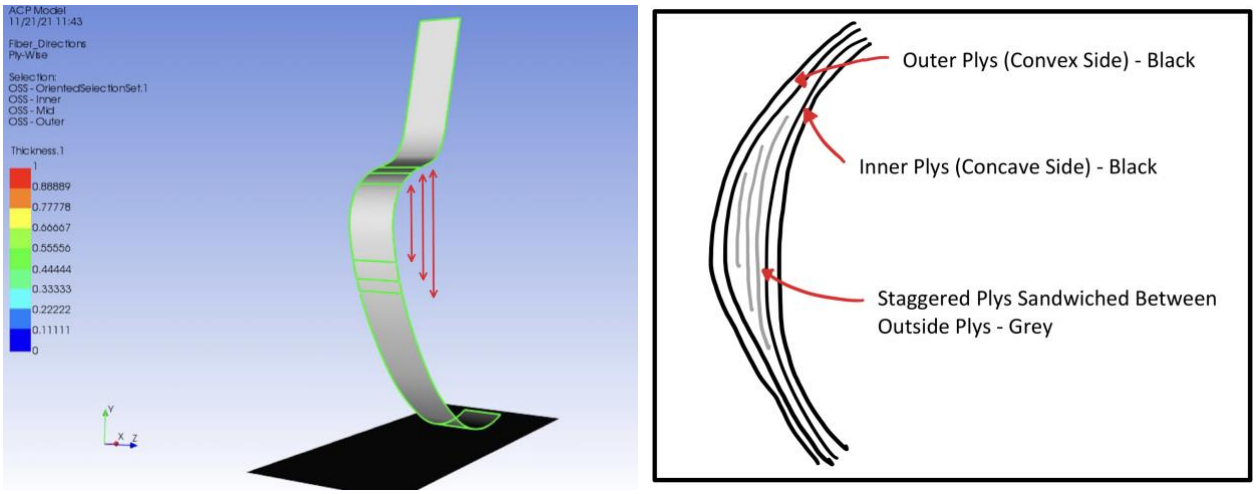

Figure 12 Staggered ply around edge of corner curvature.

In ACP, named selections were defined for the staggered sections to control the layup independent of the mesh. Three staggered smaller sections were sandwiched in between ply running the entire length of the blade. The number of ply in the outside layers and each of the staggered inside layers was then parametrised such that they could be individually adjusted. For this study only [-30/0/30] UD ply was used, with the expectation that the thicker corner sections would relieve the fringe effect failure points as seen in the second study. The results of this study were summarised in the table overleaf.

Design Number	Number of [-30/0/30] laminae/plys					Max Stress (MPa)	Safety factor	Max Total Thickness (mm)	Min Total Thickness (mm)
	Convex (Outer) Edge	Concave (Inner) Edge	Taper Section 1 (smallest)	Taper Section 2	Taper Section 3 (largest)				
DP 0	12	12	3	3	3	303.1	0.59	19.8	14.4
DP 1	13	13	4	4	4	253.8	0.86	22.8	15.6
DP 2	13	13	3	4	5	252.1	0.85	22.8	15.6
DP 3	14	14	3	4	5	216.3	1.14	24	16.8
DP 4	14	14	3	3	3	220.0	1.15	22.2	16.8
DP 5	14	14	2	3	5	216.9	1.13	22.8	16.8
DP 6	14	14	5	3	2	227.9	1.10	22.8	16.8
DP 7	14	14	4	4	3	219.3	1.16	23.4	16.8
DP 8	15	15	3	3	3	190.4	1.47	23.4	18
DP 9	15	15	2	2	2	217.6	1.37	21.6	18
DP 10	14	15	3	3	3	204.4	1.31	22.8	17.4
DP 11	15	14	3	3	3	205.7	1.30	22.8	17.4

Table 5 Parametric study 4 - Staggered Inner Plys

The study revealed several interesting points. Firstly, an even distribution of the number of plys across all three inside layers performs better than an increasing or decreasing number of plys through these three layers. This can be observed in the difference between designs DP 1 and DP 2 and again with DP 4 and DP 5. Furthermore, a relatively small number of sandwiched staggered plys also performed better. The iteration DP 9 was chosen as the best performing, with a SF of almost 1.5. The minimum total thickness of 18mm is the thickness where there are no staggered plys and the maximum total thickness refers to the thickness at the middle of the curvature. Figure 13 shows a graphical representation of these results.

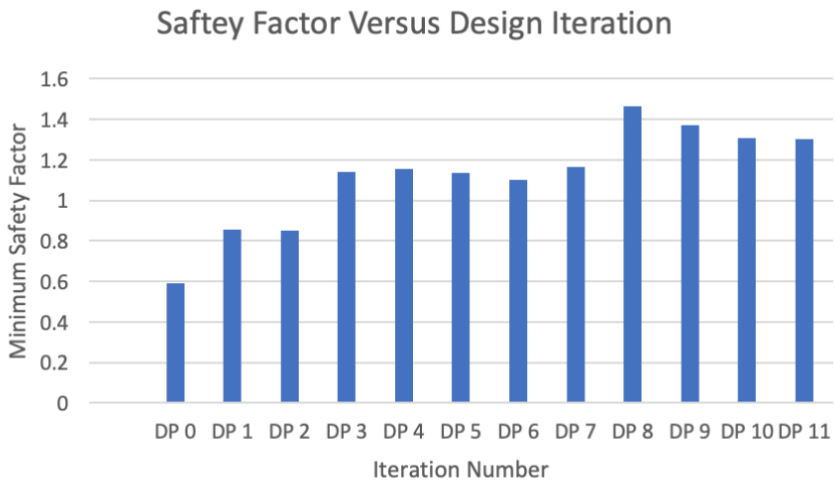

Figure 13 Graph of Design Iterations

7. Concluding Remarks & Future Work

The methods in this report appear to have given a robust analysis of the stresses exhibited in an adapted model of the Össur™ Cheetah Xcel running blade. The discretisation scheme was appropriately shown to converge at certain element size, and the preliminary isotropic study was accurately used to validate the loading and boundary conditions of the model in a static structural analysis, with only little deviation to hand calculated stress results.

Four individual parametric studies were conducted using different layup configurations of carbon fibre fabric indicating several interesting results. Carbon fibre twill in a [0/45] quasi-isotropic arrangement actual outperformed a unidirectional [-30/0/30] arrangement despite the unidirectional fibre being stronger in the orientation of the bending stresses experienced. Noticeable fringe effects could be seen with the unidirectional fibre which caused it to fail along the edges of the blade. The most favourable design was selected from the last parametric study with a Safety Factor of 1.47, blade thickness of 18mm and 23.4mm at the middle of the curved section of the blade. The design could still be further optimised by finding the optimal configuration of fibres running lengthwise along the blade and across it, such that the stress is spread evenly along the width and failure doesn't occur only along the edges of the blade. For example, 90˚ UD fibres could be incorporated to hold the blade together and spread the stress through the thickness. A further study using staggered plys could also be conducted using the quasi-isotropic layup and compared to the unidirectional case. Furthermore, the Cheetah Xcel running blade is not only variable in thickness, but its width is also not constant. This is an additional variable that could be investigated. Additional extensions to this analysis could include investigating the bolted joint at the attachment point of the blade or topology optimising the aluminium L-bracket. Different loading conditions such as a heel, toe strike and sideward angled impact should also be investigated.

Notably, the thinnest blade that could be optimised in this study was between 18mm and 23.4mm, whereas the Össur blade is on average approximately 13mm thick. This difference could further be attributed to the generous loading conditions in this investigation already having inbuilt margins of safety. Furthermore, stronger carbon fibre fabric than the 230GPa fabric may have also been used in the Össur blade. Nonetheless, the aim of this investigation has been fulfilled as the simplified model of the Össur blade could be accurately simulated in the ANSYS Composite PrepPost and optimised over various iterations.

8. Works Cited

[1] L. Greenemeier, “Blade Runners: Do High-Tech Prostheses Give Runners an Unfair Advantage?,” *THe Scientific American,* 2016.

[2] S. J. Andrew Miner, “Design, Testing, Analysis, and Material Properties of Carbon Fiber Reinforced Polymers,” *Rose-Hulman Undergraduate Research Publications ,* 2016.

[3] F. N. Cogswell, THermoplastic. Aromatic Polymer Composites, London: Butterworth Heinemann, 1992.

[4] OSSUR, “Cheetah® Xcel,” 2021. [Online]. Available: https://www.ossur.com/en-au/prosthetics/feet/cheetah-xcel?tab=specification.

[5] D. M. H. F.-A. Saleel Hussein Abood, “Analysis of Prosthetic Running Blade of Limb Using Different Composite Materials,” *University of Baghdad Journal of Engineering,* 2019.

[6] E. Pitsiougka, “Can we use 3D elements for bending problems?,” 2019. [Online]. Available: https://www.researchgate.net/post/Can-we-use-3D-elements-for-bending-problems.

[7] S. J. Andrew Miner, “Design, Testing, Analysis, and Material Properties of Carbon Fiber Reinforced Polymers,” *Rose-Hulman Undergraduate Research Publications,* 2016.

[8] A. B. a. M. G. Frank Sup, “Design and Control of a Powered Transfemoral Prosthesis,” *US National Library of Medicine National Institutes of Health,* vol. 27, 2009.

[9] S. M. A. a. A. I. Kubba, “Fatigue Characteristics and Numerical Modelling Prosthetic for Chopart Amputation,” *Modelling and Simulation in Engineering,* vol. Volume 2020, 2020.

[10] OSSUR, “Cheetah® Xcel,” 2021. [Online]. Available: https://www.ossur.com/en-au/prosthetics/feet/cheetah-xcel.

[11] A. K. P. a. G. R. Mero, “Biomechanics of sprint running,” *Sports Medicine,* vol. 13, pp. 376-392, 1992.

9. Appendix A – Hand Calculations

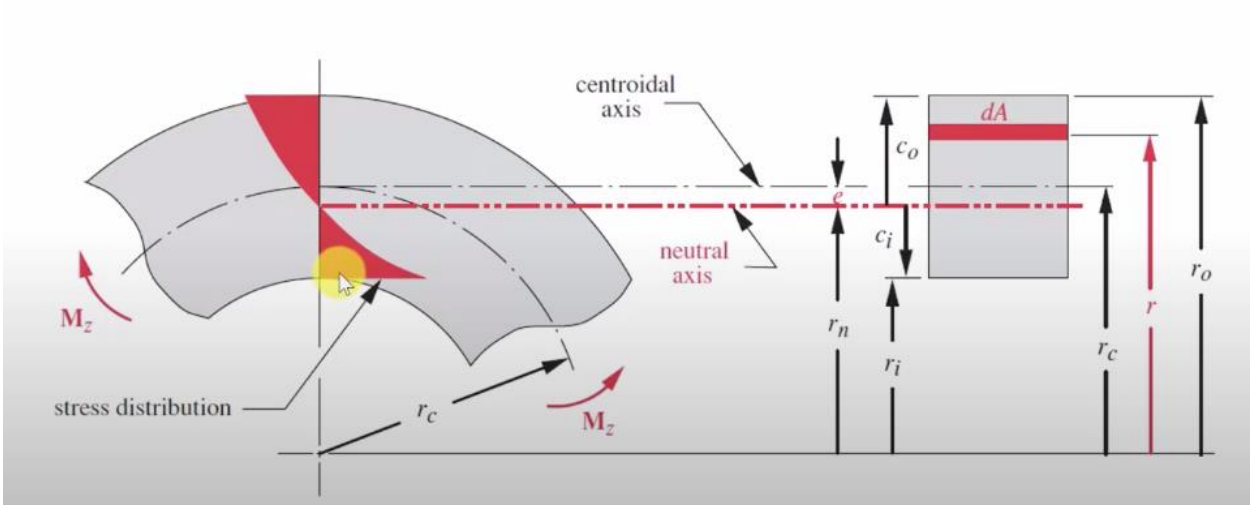

Figure 14 Diagram of variable definition

The following formulas can be applied for the combined axial and bending stress at the inner σ_i and outer σ_o fibres of the curved circular section of the blade.

$$\sigma_i = \frac{M_{min}\, c_i}{Aer_i} + \frac{F}{A} \quad ; \quad \sigma_o = \frac{M_{max}\, c_o}{Aer_o} - \frac{F}{A} \quad ; \quad e = r_c - r_n = r_i + \frac{h}{2} - \frac{h}{\ln\left(\frac{r_o}{r_i}\right)}$$

Variables:

Outer Radius	**r_o**	0.066132
Inner Radius	**r_i**	0.051132
Outer to Neutral Axis	**c_o**	0.007821199
Inner to Neutral Axis	**c_i**	0.007178801
Thickness	**h**	0.015
Width	**w**	0.06
Force Applied	**F**	1000
Minimum Moment Dist.	**x_min**	0.152792
Maximum Moment Dist.	**x_max**	0.181576
Maximum Moment Dist.	**M_max**	181.576
Minimum Moment	**M_min**	152.792
Average Moment	**M_avg**	167.184
Neutral Axis to Centroid Dist.	**e**	0.000321199

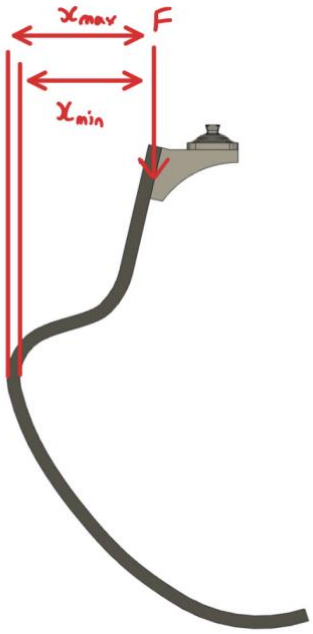

Figure 15 Figure showing moment axis

The minimum and maximum bending moment are found by multiplying the applied force by the perpendicular minimum and maximum moment arm distance respectively. The stresses are found using the equations given above.

$$\sigma_i = \frac{M_{min}\, c_i}{Aer_i} + \frac{F}{A}$$

$$= \frac{M_{min}\, c_i}{wher_i} + \frac{F}{wh}$$

$$= \frac{152.792 \cdot\ 0.00718}{0.06 \cdot 0.000321 \cdot 0.0511} + \frac{1000}{0.06 \cdot 0.000321}$$

$$= 70.946\ \text{MPa}$$

$$\sigma_o = \frac{M_{max}\, c_o}{Aer_o} - \frac{F}{A}$$

$$= \frac{M_{min}\, c_i}{wher_i} - \frac{F}{wh}$$

$$= \frac{181.576 \cdot 0.00782}{0.06 \cdot 0.000321 \cdot 0.0661} - \frac{1000}{0.06 \cdot 0.000321}$$

$$= 61.234\ \text{MPa}$$